

Fiducial Cuts for electrons in the CLAS/E2 data at 4.4 GeV

D. Protopopescu, F. W. Hersman, M. Holtrop  
University of New Hampshire, Durham, NH 03824

S. Stepanyan  
Christopher Newport University, Newport News, VA 23606

and CLAS/E2 run group

November 27, 2000

**Abstract**

The step by step procedure for deriving geometrical fiducial cuts for electrons in the data taken during the CLAS/E2 run period, with beam energy  $E = 4.4$  GeV is discussed. These data were obtained without CLAS Čerenkov counter in the Level 1 trigger of CLAS DAQ and therefore the fiducial functions derived are completely different from the functions obtained earlier for CLAS/E1 runs. Also, in the present approach, the fit function does not fix the energy bin width. By this we achieve increased flexibility and better accuracy of the cut.

## Introduction

The CEBAF Large Acceptance Spectrometer (CLAS) at Jefferson Lab is designed to measure multi-particle final states [1]. It is based on six iron-free superconducting coils that generate a toroidal magnetic field in between. Each of the six gaps between the coils is equipped with a set of drift chambers (DC) [2] and scintillator counters (SC) [3] from  $10^\circ$  to  $145^\circ$  in polar angle, and Čerenkov counters (CC) [4] and electromagnetic calorimeters (EC) [5] from  $10^\circ$  to  $45^\circ$ .

In electron scattering experiments with CLAS, the recorded event is accepted for physics analysis if the scattered electron is identified. For electron identification, in most cases, valid signals in all four detectors are required. Electron detection efficiency around the mid plane in each sector is reproducible in the GEANT (GSIM) simulations. Due to the complicated readout structures of EC and CC, detection and reconstruction efficiencies are not well understood in the regions close to the torus coils, and close to the dead channels of detector elements. In order to minimize systematic uncertainties in the physics analysis it is important to accept events in the fiducial region of the detector, where efficiencies are understood.

Fiducial cuts for electrons in  $ep$  scattering experiments were derived earlier by V.Burkert *et. al.* [6] for the CLAS/E1 runs. These cuts define a region in the production  $(\theta, \phi)$  space for a given momentum, where detection efficiency is almost constant on  $\phi$  and can be reproduced in simulations. Although these functions should, in principle, scale with momentum and the magnetic field, it is not always possible to use the same function due to different run conditions (bad channels, target position, trigger, etc.).

Data taken at beam energy  $E_o = 4.4$  GeV during the CLAS/E2 run do not have Čerenkov counters in the Level 1 trigger of the CLAS DAQ. The main motivation for excluding CC from the trigger is that a lot of E2-related physics proposals are focused around the kinematics of quasi-elastic, dip and  $\Delta$  production regions, starting from momentum transfer  $Q^2$  as low as possible. Scattered electron momentum in these conditions is generally above the pion threshold in CC, and  $e/\pi$  rejection relies on forward electromagnetic calorimeters only. Excluding CC cut from electron identification makes the fiducial region very different from the previously defined region for E1. In this report we describe the procedure for electron selection and determination of the fiducial volume of the detector without Čerenkov counters.

## Our Method

We define a “cut” as a two-dimensional doubly-curved surface passing through the three-dimensional  $(p, \theta, \phi)$  space, enveloping the region that satisfies certain selection criteria. In our case, as we stated above, the criterion would be “uniform acceptance”. We define apriori our “uniform acceptance” plateau as the region contained between the steep rise and the sudden drop on a counts vs.  $\phi$  histogram drawn at given  $p$  and  $\theta$ ”.

To determine the equation of the cut surface, we do the following:

1. select “good” electrons with cuts on the forward electromagnetic calorimeter (EC)
2. select the flat acceptance regions for small bins of momenta in the  $\theta$  and  $\phi$  space.
3. fit the final coefficients with smooth functions of  $(p, \theta$  and  $\phi)$ .

As a note to the reader: frequent references in this text point towards the web-based documentation ([7] and [8]). The website contains complete documentation, programs and *all* the graphics to illustrate the procedure. Some file names are given in the text in the event that the reader would like to customize our codes and procedure for his(hers) fiducial cuts.

## Step One: Forward Calorimeter Cut

As was mentioned above only forward EC information will be used for electron identification. Since the ratio of the deposited energy in EC to the momentum of the particle measured in DC ( $E_{EC}/p$ ) is the main tool for  $\pi/e$  rejection, we will define the fiducial region as *a region where the electron distribution is constant on  $\phi$  after the cut on deposited energy*. Consequently, regions where due to shower leakage measured energy is less than it should be are eliminated. (There are other cuts that will be used for final electron selection, like energy depositions in the inner and outer parts of EC, or the width of a shower. These quantities remain stable in the fiducial region defined above.)

The scintillators in the forward electromagnetic calorimeter are grouped in three planes, denoted as U, V and W. The scintillator bars in the U plane have an orientation perpendicular to the beam axis, while the scintillators in the V and W planes are rotated by  $120^\circ$ . In Fig.1 the distribution of electrons on the calorimeter sides is shown. This defines a natural system of coordinates that is the most convenient to use for defining geometrical cuts.

It is useful to study the variation of the ratio  $E_{EC}/p$  versus calorimeter coordinates. Such a plot is shown in Fig.2, with  $p > 0.9$  GeV. Plots for certain energy subranges are available for reference in [7].

As a first step electrons with  $E_{EC}/p \geq 0.2$  will be selected (see Fig.2). In Fig.3 a magnified plot of the above mentioned distribution is shown. For clarity, only electrons with momentum  $p > 3.0$  GeV are kept here, given that electrons with momentum in this range are detected mainly at forward angles, and are more sensitive to our  $uvw$  cut.

It is seen that in the regions  $v \geq 371$  and  $w \geq 407$ , the ratio  $E_{EC}/p$  drops dramatically. This is due to the electron shower leakage out of the sides of the calorimeter. Similar plots had been made for individual sectors and they are available in [7]. Cuts on the edges  $u > 20$  cm,  $v < 371$  cm and  $w < 407$  cm were applied to select events with  $E_{EC}/p > 0.2$  GeV. (It was concluded that using different cuts for each sector was not necessary.) Figure 4 shows such a cut ( $u > 20, v < 371, w < 407$  and  $E_{EC}/p > 0.2$ ).

We have studied the behavior of the  $E_{in}/E_{out}$  ratio versus the EC coordinates (with  $E_{in}$ ,  $E_{out}$  being the energy loss in the inner and the outer parts of the EC, respectively). But, as it can be found in [7], these quantities do not depend on the position on EC, after the above cuts.

Our final criteria for the preparatory cuts would then be:

$$u > 20, v < 371, w < 407, E_{EC}/p > 0.2 \tag{1}$$

Figure 5 illustrates how this  $uvw$  cut reflects onto the energy spectrum of the electrons that we detect.

The conditions in equation (1) are imposed on the data used to derive the fiducial cut, to select a set of well identified electrons. They will not explicitly show in the final cut, which is purely geometrical. Also, in the physics analysis, data below 0.9 GeV and  $16^\circ$  in  $\theta$  will be discarded, since this is below the trigger threshold and is clearly outside of the acceptance region of CLAS.

## Step Two: Finding the Uniform Acceptance Region

After we have selected “good” electrons, as described in the previous section, we proceed to study the dependence of the detector acceptance on angles and energy.

Figure 6 shows some typical  $(\phi, \theta)$  plots after the forward calorimeter cut has been applied.

The energy range was divided in small bins and then for each energy bin and for each sector two-dimensional distribution of events in  $\theta$  and  $\phi$  plane is studied. In figure 7 a number of such distributions are presented. Regions with black points were cut out with cuts described above. The energy bin width is set to 100MeV. The energy bin  $n$  is defined as the range between  $0.1 \times n$  and  $0.1 \times (n + 1)$  GeV.

The histograms in Fig.6 exhibit a well contoured semicircular region, surrounded by a fuzzy region. We want to select this solid area of the histogram, which is the flat acceptance region, and discard the blurred area surrounding it. For this, we will fit its contour with a function  $\phi(\theta, E_n, s)$ , where  $E_n$  is the energy bin,  $s$  the sector and  $\theta$  the angle.

Of course, before this, one needs to accurately define what means “flat”. For this purpose, what we do is slice these two-dimensional plots in theta bins<sup>1</sup> of 1°, and fit these histograms with a trapezoidal function.

The function used is:

$$y = \begin{cases} p_4(x - p_2)/(p_0 - p_2) & \text{if } p_2 \leq x < p_0 \\ p_4 & \text{if } p_0 \leq x \leq p_1 \\ p_4(x - p_3)/(p_1 - p_3) & \text{if } p_1 < x \leq p_3 \\ 0 & \text{if } x < p_2 \text{ or } x > p_3 \end{cases} \quad (2)$$

Some typical trapezoids (fitted  $\theta$ -slices) are shown in Fig.8. More can be found in [7]. Now, on these plots, the top horizontal side of the trapezoid is our “flat” acceptance region.

We found the procedure to give us reliable results in over 90% of the fits. The procedure is automatic and the code used (`concat.cc`) can be found in [8]. The few bad fits that occurred were not corrected manually, because the results (parameters) of these first generation fits are fitted as a function of  $\theta$  afterwards. This way, both statistical and procedural errors are automatically minimized.

The coordinates of the edges of the top of the trapezoid, for each energy bin and sector are written to a file named `fiducial_00.dat`. This is a text file organized on six columns, each row containing the following: a version stamp, the energy bin number,  $\theta$  bin, sector number,  $p_0$  and  $p_1$ , where parameters  $p_0$  and  $p_1$  are the coordinates of the edges of the top of the trapezoid (see Fig.8).

Then we use another code (`fcfit.cc` [8]) to fit these points with a function  $\phi = \phi(\theta, E_n, s)$ , for every energy bin and sector. The procedure is completely automatic.

The function  $\phi = \phi(\theta, E_n, s)$  that most accurately describes the contours in Fig.6 is [9]:

$$\phi(\theta) = \begin{cases} b(1 - ((\theta - t_0)b/a + 1)^{-1}) & \text{if } t_0 < \theta < t_1 \\ 0 & \text{otherwise} \end{cases} \quad (3)$$

where the coefficients  $a, b, t_i$  contain the dependency on  $E_n$  and  $s$ . The actual angle  $\phi$  is obtained by scaling this formula for each sector:

$$f_{0,1}(\theta, E_n, s) = 60(s - 1) \mp \phi(\theta) \quad (4)$$

where the sign  $+$  stays for the upper branch (with coefficients  $a_1, b_1, t_0, t_1$ ) and the  $-$  sign is for the lower (described by  $a_0, b_0, t_0, t_1$ ).

A plot illustrating this step is in Fig.9. These second generation set of parameters are saved into the file `fiducial_01.dat`, which is organized as follows: each row contains a version stamp, energy bin number, the limits  $t_0$  and  $t_1$  and the  $a_0, b_0, a_1, b_1$  curvature and width parameters for the lower and upper halves, respectively (please see equations (3) and (4) and Fig.9).

### Step Three: Smooth It

What is new in the present procedure of deriving the fiducial cuts is that we did not limit ourselves to obtaining a set of empirical values but we tried to find a systematics that would give us a consistent set of parameters.

---

<sup>1</sup>bin  $n$  is from  $n$  degrees ( $^\circ$ ) to  $(n + 1)$  degrees

We have obtained 62 different 4-parameter functions  $\phi = \phi(\theta, s)$ , one for each sector and energy bin considered. Next, we want to fit the coefficients of these functions in order to obtain a smooth function  $\phi = f_{0,1}(\theta, E, s)$  that is to be included in our `TE2AnaTool` package for current use in analysis. For this, we have another code, `fc2fit.cc` [8], that reads the output tables of the previous step to produce the final parameter file.

We remind the reader that the function in equation (3) is used to define the acceptable angular range  $(\phi, \theta)$  for the detected electron. In the present approach, we did not require that the accepted region is symmetric with respect to the mid-plane of the sector, so we have two sets of parameters  $a, b$  for each energy bin and sector (upper and lower halves in Fig.9).

One believes that the first two parameters,  $t_0$  and  $t_1$ , should reflect the geometry of the detection system. The parameters  $a$  and  $b$  are related to the range in  $\phi$  that is acceptable for defined values of  $\theta$ , i.e. to the geometry of our detector. Thus, we expect that the variation of these coefficients with the energy  $E$  must be smooth. In figure 10, one finds evidence that these dependencies can be described by smooth functions.

The fitting procedure that gives us the final set of parameters  $t_0, t_1, a_0, b_0, a_1$  and  $b_1$  is completely automatic. To describe the energy dependence of  $t_0$  and  $t_1$  we use a power function:

$$t_i = c_{1i} E^{c_{2i}} \quad i = 0, 1 \quad (5)$$

and for the other four parameters a polynomial function of degree five:

$$P_5(E) = \sum_{n=0}^5 c_n E^n \quad (6)$$

However, in the final version of the code, there is a switch that one can use to set always the lower limit for  $t_1$  at  $45^\circ$ , which is actually the hardware limit on  $\theta$  in the EC for straight tracks.

The third generation parameters all go into a file named: `fiducial_02.par`, that is read at initialization by the routine `SetFiducialCutParameters()`, included in the `TE2AnaTool` package. This file is organized on eight columns: first is a tag, second is the sector number, and the next six are the coefficients of the functions in equations (5)<sup>2</sup> and (6).

Figure 11 shows the overall result of the fiducial cut as made by using the final version of the routine. Please notice the narrowing in the forward region.

In some sectors (see Fig.11), we notice some small gaps. These are better corrected for in a separate procedure that eliminates faulty scintillators and bad DC regions, therefore, the present version of fiducial cuts procedure does not contain this feature. Figure 12 shows some energy bins after the fiducial cut.

It is interesting to see the energy distribution of the scattered electron after these cuts. Figure 13 compares the shape of the distributions at various stages of our procedure. Let us take a look at it: we lose quite a lot of data with the  $uvw$  cut, but, again, this is “bad” data. The  $E_{EC}/p$  condition cuts out even more, but we see that it doesn’t bias the final distribution.

We notice a disproportionate loss of high energy electrons that is explained by the forward peaking of the high energy electrons, at angles where the CLAS acceptance is small, not flat and hence cut out by the fiducial cuts. Therefore, we would need more detailed methods for obtaining our acceptance function at energies above 3.5 GeV.

## Summary

We prepared the terrain with the forward calorimeter cut, eliminating by this the electrons that were

---

<sup>2</sup>obviously, only two of the rows corresponding to the power functions contain nonzero values

not properly detected. We split the angle-energy range in small bins and find the contour of the region of interest, that is *the constant acceptance* plateau. We get from this a set of curves. What is inside the contour passes as OK, what is out is discarded.

Further, we wanted to eliminate the constraint of a fixed bin width, which is not very convenient if we want to ensure flexibility of the analysis software. Hence, we fitted each of the *coefficients* of these functions with a function depending only on energy and sector number. The parameters of the latter functions were saved in a file destined to the CLAS\_PARMS directory or the database.

Somewhere at the beginning of his(hers) analysis code, the user must initialize the fiducial cut function by calling **SetFiducialCutParameters()**, which reads the values from the PARMS file mentioned above.

Then, what our **EFiducialCut(p)** function does for an event characterized by momentum  $p$  and angles  $\theta$  and  $\phi$ , is calculating the coefficients  $c_i(E)$  (where  $c_i$  stands for  $\{t_0, t_1, a_{0,1}, b_{0,1}\}$ ), and inserting them into the contour functions  $\phi = f_{0,1}(c_i, \theta)$ . If our  $\phi$  is contained in the interval  $(f_0(E, \theta), f_1(E, \theta))$ , the event is accepted, else the event is rejected.

The user must call the function **EFiducialCut(El3Vect)** in a conditional statement, where the argument **El3Vect** passed is the electron momentum 3-vector.

## Acknowledgements

One of the authors (D.P.), would like to thank to Prof. Larry Weinstein (ODU) for ideas and critical observations and to Gagik Gavalian (UNH) and Bin Zhang (MIT) for fruitful discussions. D.P. is also grateful for the inspiring environment that the Nuclear Physics Group of UNH offered to him during the work on this project.

## References

- [1] B. Mecking et al., *CLAS detector*, In preparation, to be submitted to Nucl. Instr. and Meth.
- [2] M.D. Mestayer et al., *The CLAS drift chamber system*, Nucl. Instr. and Meth. **A449** (2000), p81.
- [3] E.S. Smith et al., *The time-of-flight system for CLAS*, Nucl. Instr. and Meth. **A432** (1999), p265.
- [4] *The Cherenkov counter system for CLAS*, In preparation, to be submitted to Nucl. Instr. and Meth.
- [5] L.C. Smith et al., *The CLAS forward electromagnetic calorimeter*, Accepted for publication in Nucl. Instr. and Meth..
- [6] Private communication
- [7] Fiducial Cuts for CLAS at 4.4 GeV, D.Protopopescu, July 2000, documentation in html format, <http://einstein.unh.edu/protopop/FiducialCuts/fc4E2.html>
- [8] C++ code bank, by D.Protopopescu, available on web at [http://einstein.unh.edu/protopop/cpp\\_codes.dir/cpp4E2.html](http://einstein.unh.edu/protopop/cpp_codes.dir/cpp4E2.html)
- [9] Zhang, B., private communication

## Abbreviations used in text

1. TJNAF is the acronym of Thomas Jefferson National Accelerator Facility
2. GSIM is the CLAS version of the GEANT Simulation Package
3. EC stands for **E**lectromagnetic **C**alorimeter, but we understand by it the forward calorimeter only. For the Large Angle Calorimeters we use the acronym LAC

## List of Figures

1	Range of the calorimeter coordinates $u, v, w$ . Dimensions on abscissa are in centimeters. . . . .	7
2	Ratio $E_{EC}/p$ plotted versus each of the three calorimeter coordinates. All $p > 0.9$ GeV are considered here. For specific subranges please see [7]. Dimensions on abscissa are in centimeters. . . . .	8
3	Magnified view of the edges of the histogram in Fig.2 with a $p > 3.0$ GeV cut applied. One can easily notice the dramatic drop of the ratio $E_{EC}/p$ near the edges. Plots for each sector can be found in [7]. Dimensions on abscissa are in centimeters. . . . .	9
4	Result of the cut on $u, v$ and $w$ . Dimensions on abscissa are in centimeters. . . . .	10
5	Energy spectra of the electron before (1) and after (2) the forward calorimeter cut as given by equation (1). $E_{el}$ is in GeV. . . . .	11
6	Some typical plots of $\phi(\theta)$ dependency. For the rest, please consult reference [7] . . . . .	12
7	Two dimensional histograms (counts vs $\theta$ - $\phi$ ) showing the overall effect of the forward calorimeter cut. Black points show what is discarded by the cut. For more details, please consult [7]. . . . .	13
8	Trapezoids fitted on histograms counts vs $\phi$ angle. We call the top "flat". Some typical examples. All the others can be found in [7]. . . . .	14
9	Second generation fit. Energy bin 10 means $1.0 \text{ GeV} < p_{el} < 1.1 \text{ GeV}$ . All other plots can be found in [7].	15
10	Third generation fits. Each fit corresponds to one of the parameters in eq.(3). Only data for sector 4 is shown. For the others sectors, please consult [7] . . . . .	16
11	Overall result of the cut. One can see that an asymmetrical shape resulted in some sectors. The fuzzy edges are due to bin overlap. . . . .	17
12	Typical plots illustrating the result of the cut. Please notice that some are asymmetrical. For more, please consult [7] . . . . .	18
13	Electron energy spectra at various stages of the procedure: before applying any cut (1), after the uvw cut (2), after the EC cut on $uvw$ and $E/p$ (4), final (3). On the last one, the region $p < 0.9$ GeV is ignored. $E_{el}$ is in GeV. . . . .	19

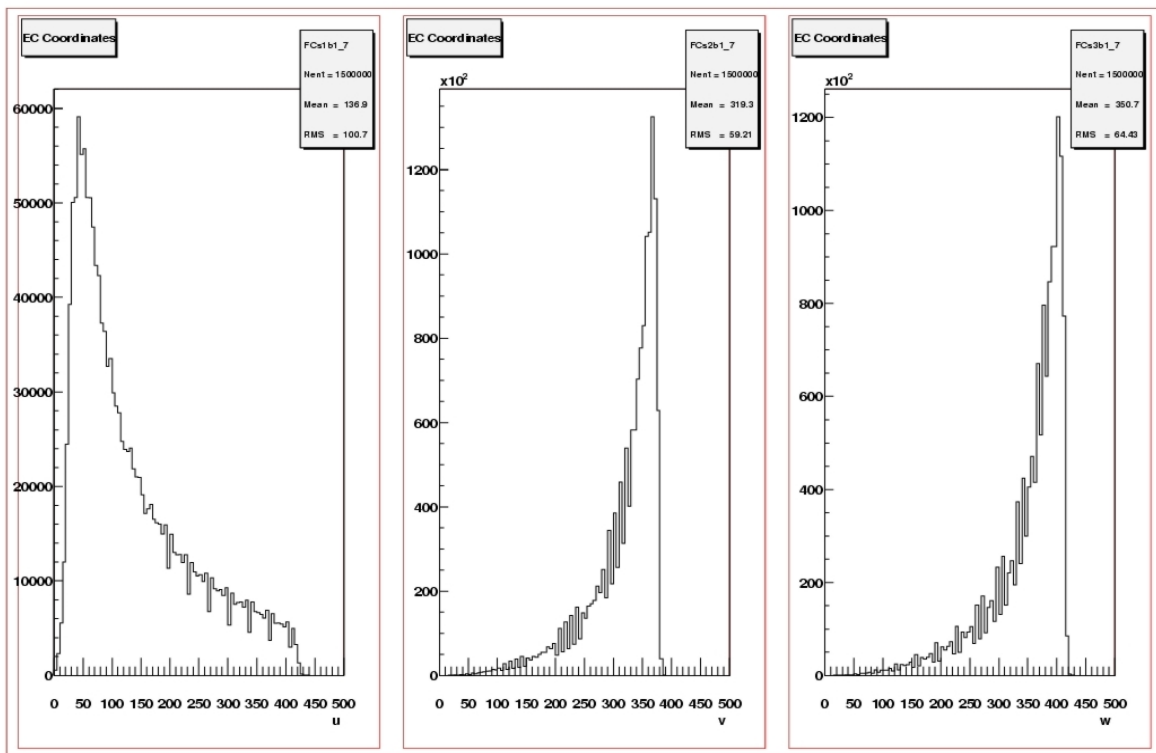


Figure 1: Range of the calorimeter coordinates  $u, v, w$ . Dimensions on abscissa are in centimeters.



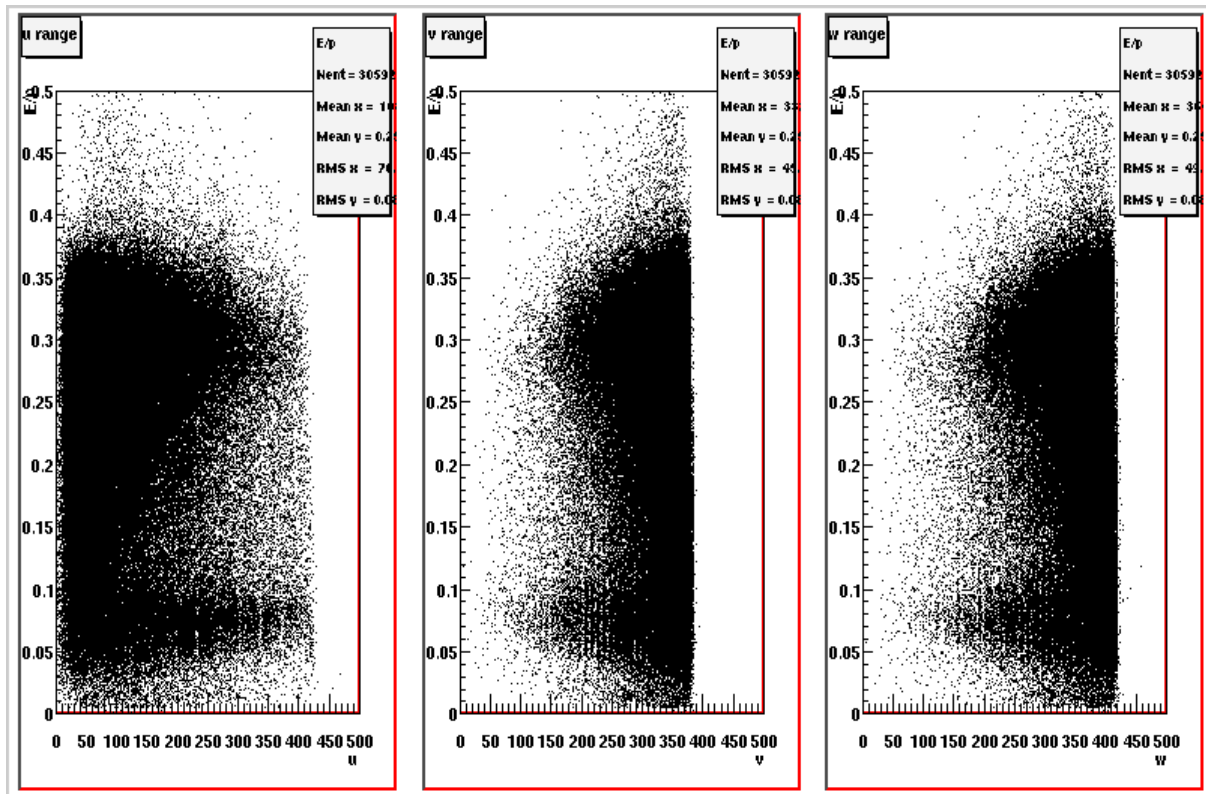


Figure 2: Ratio  $E_{EC}/p$  plotted versus each of the three calorimeter coordinates. All  $p > 0.9$  GeV are considered here. For specific subranges please see [7]. Dimensions on abscissa are in centimeters.

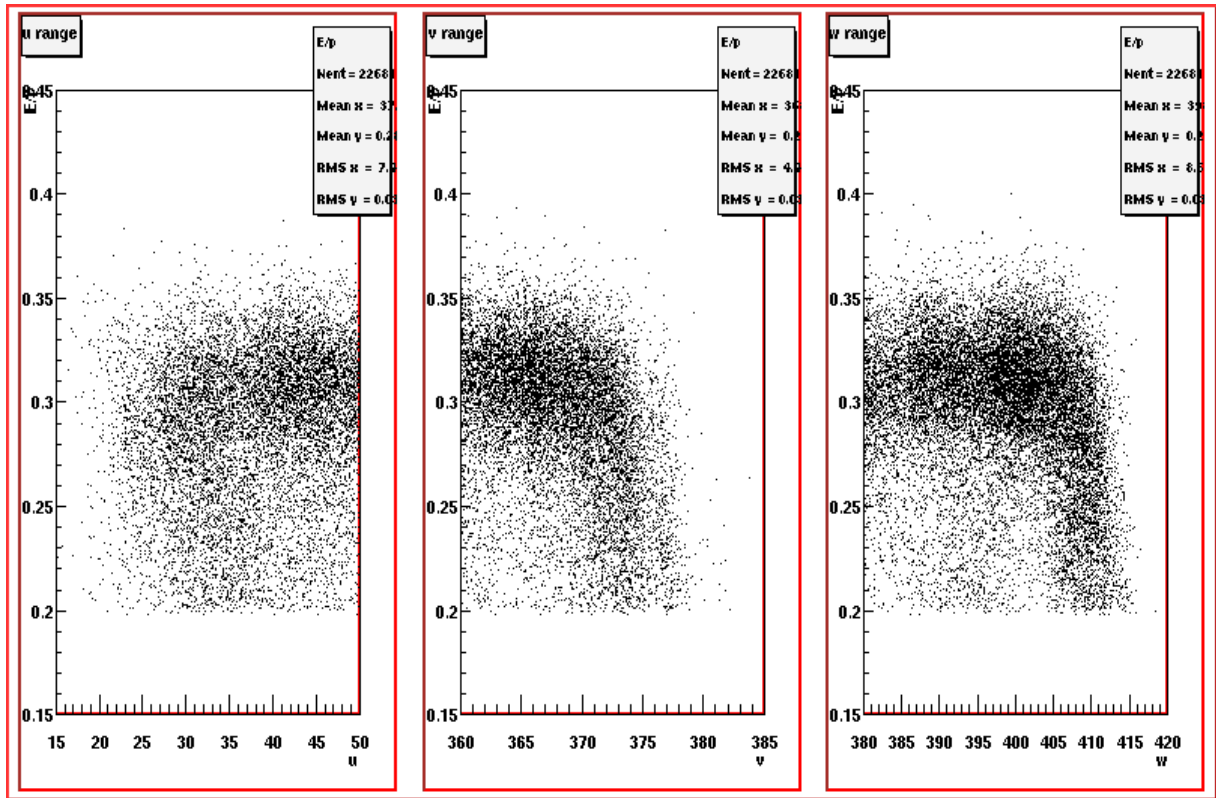


Figure 3: Magnified view of the edges of the histogram in Fig.2 with a  $p > 3.0$  GeV cut applied. One can easily notice the dramatic drop of the ratio  $E_{EC}/p$  near the edges. Plots for each sector can be found in [7]. Dimensions on abscissa are in centimeters.

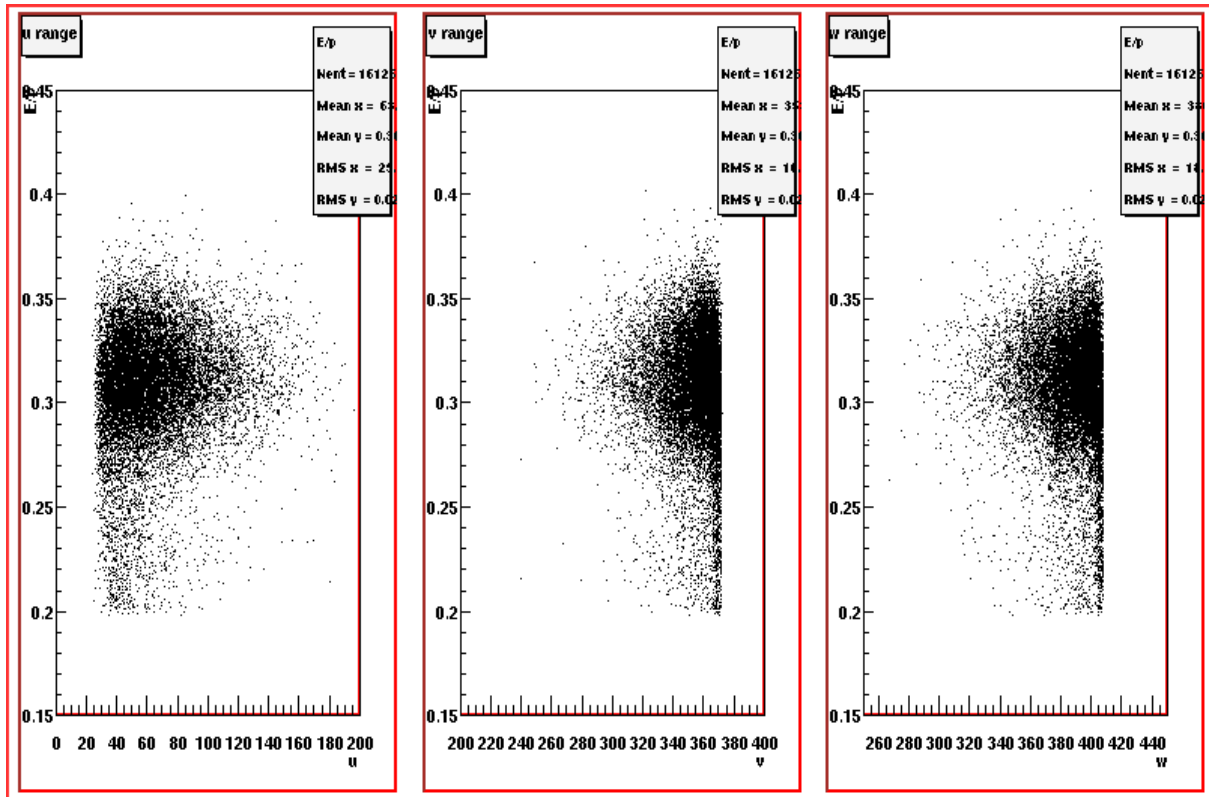


Figure 4: Result of the cut on  $u, v$  and  $w$ . Dimensions on abscissa are in centimeters.

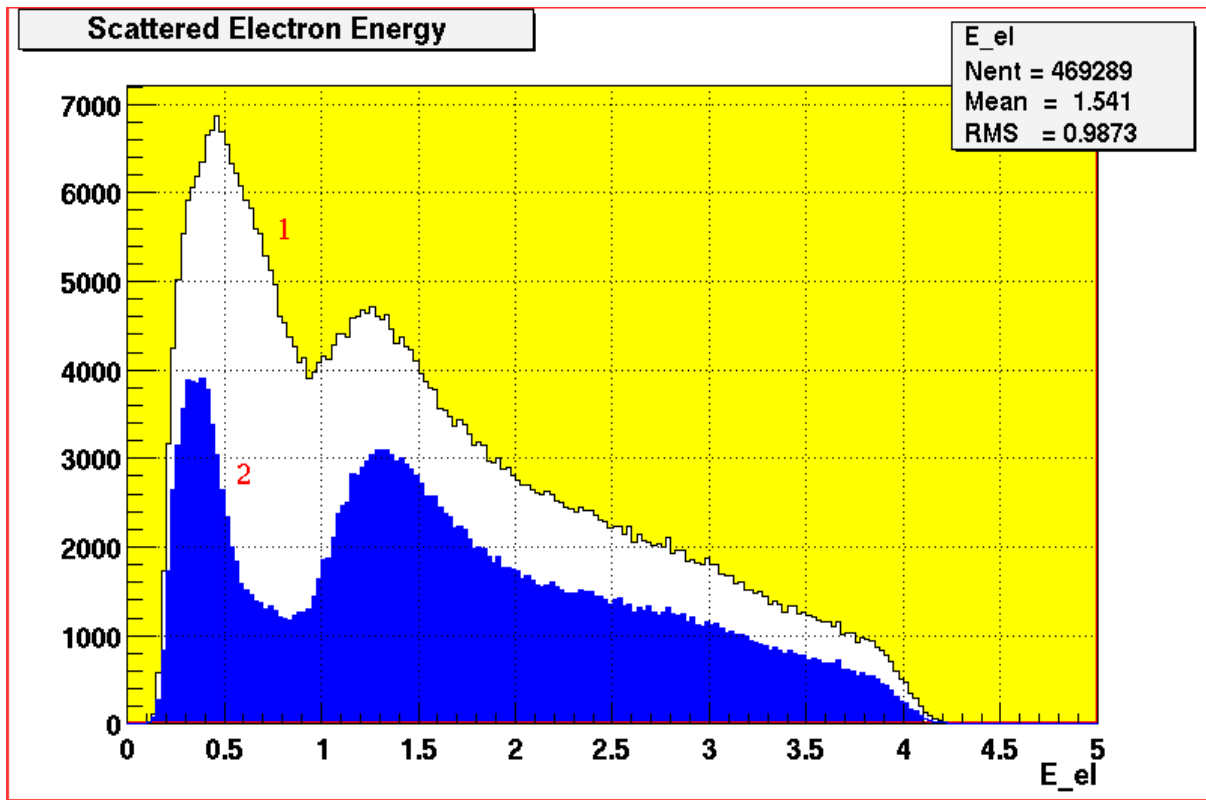


Figure 5: Energy spectra of the electron before (1) and after (2) the forward calorimeter cut as given by equation (1).  $E_{el}$  is in GeV.

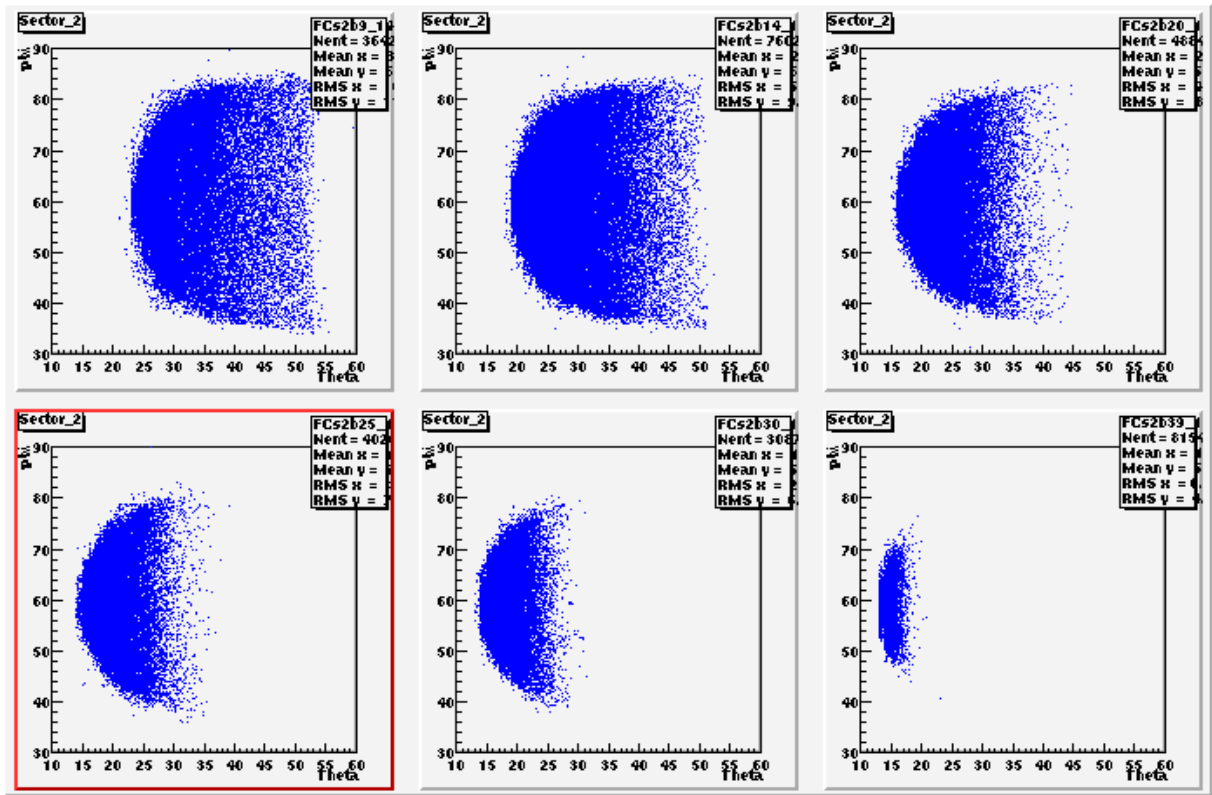


Figure 6: Some typical plots of  $\phi(\theta)$  dependency. For the rest, please consult reference [7]

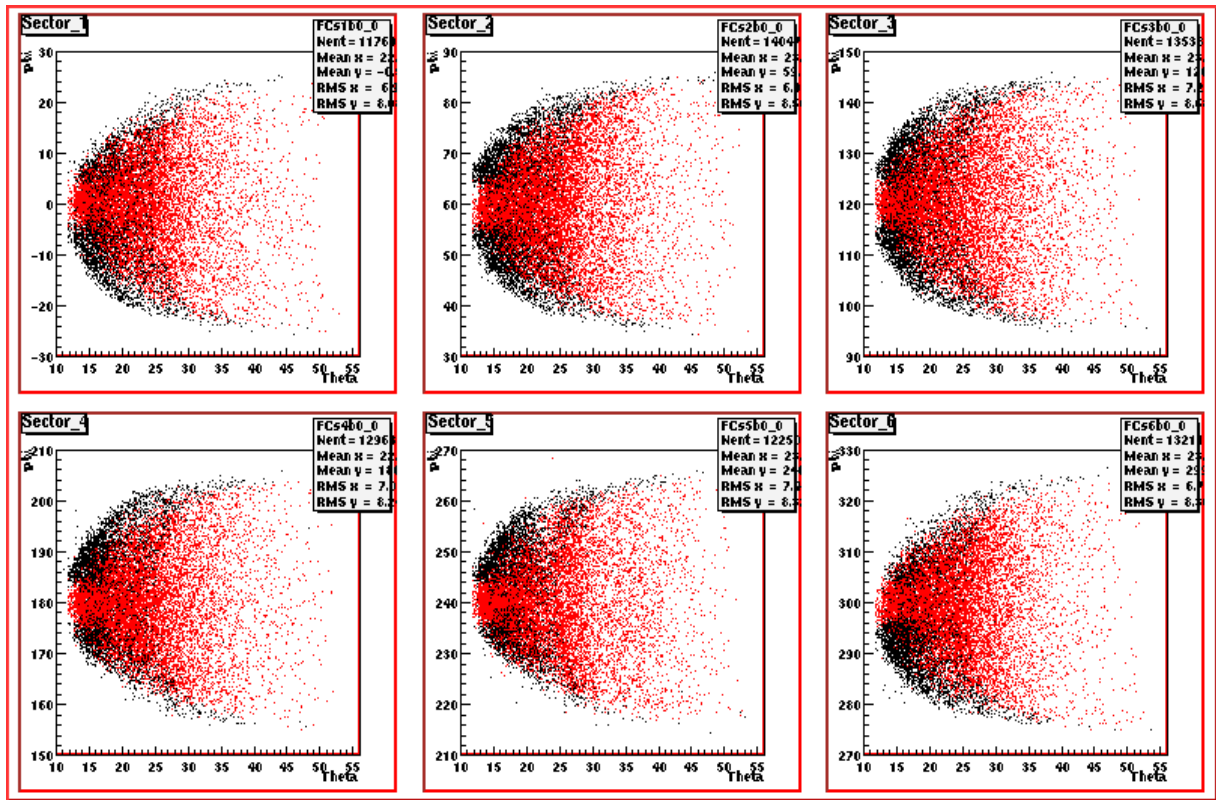


Figure 7: Two dimensional histograms (counts vs  $\theta$ - $\phi$ ) showing the overall effect of the forward calorimeter cut. Black points show what is discarded by the cut. For more details, please consult [7].

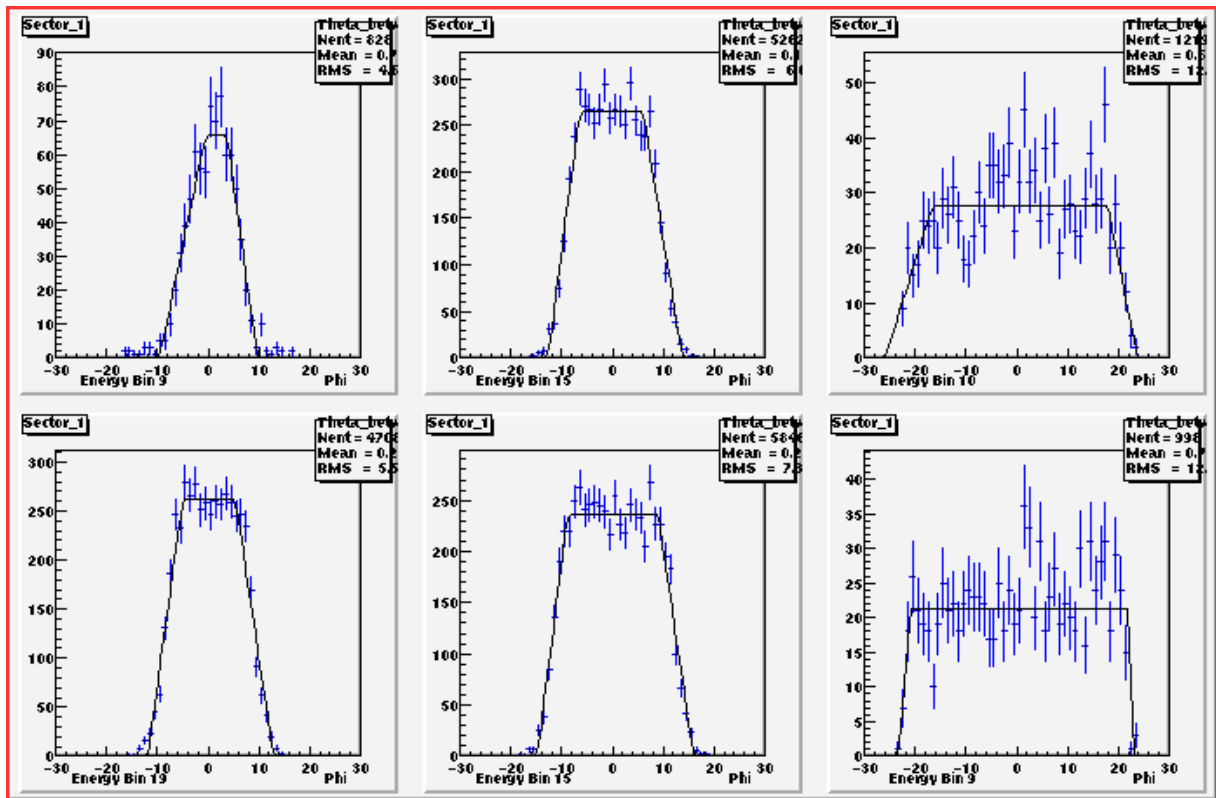


Figure 8: Trapezoids fitted on histograms counts vs  $\phi$  angle. We call the top “flat”. Some typical examples. All the others can be found in [7].

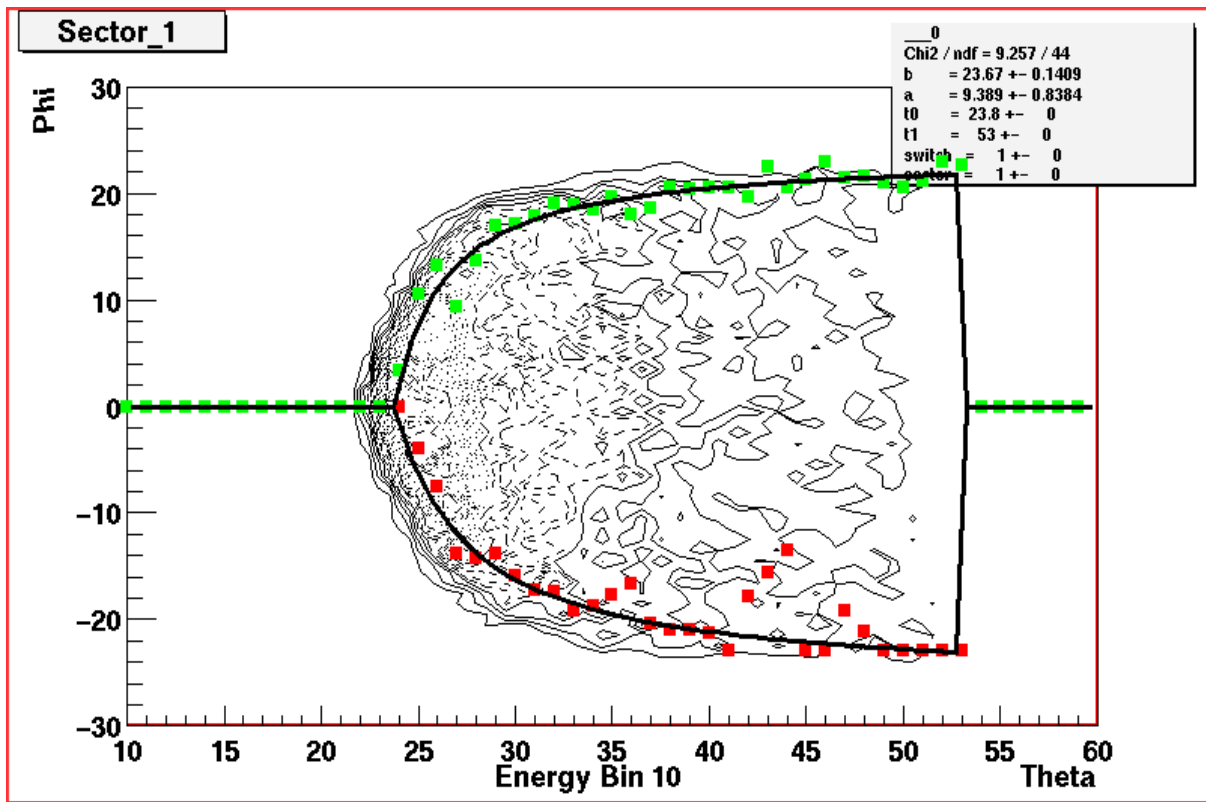


Figure 9: Second generation fit. Energy bin 10 means  $1.0 \text{ GeV} < p_{el} < 1.1 \text{ GeV}$ . All other plots can be found in [7].



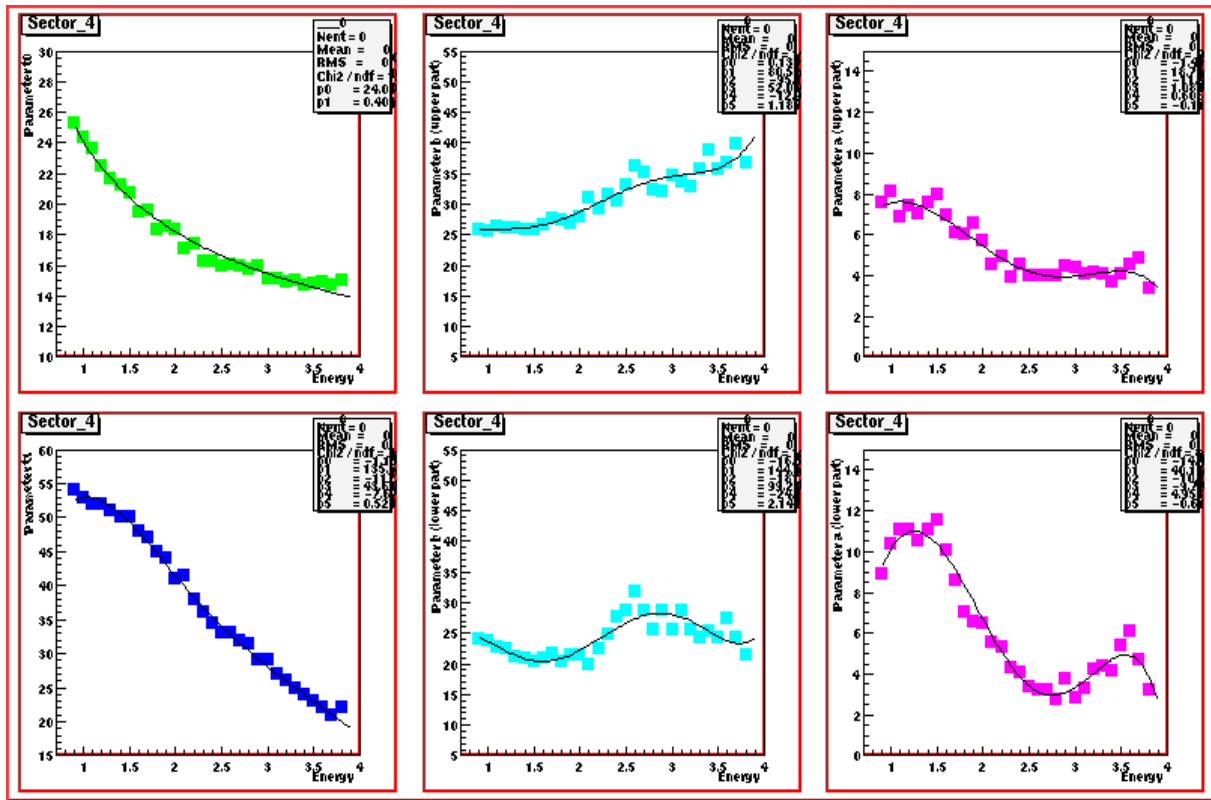


Figure 10: Third generation fits. Each fit corresponds to one of the parameters in eq.(3). Only data for sector 4 is shown. For the others sectors, please consult [7]

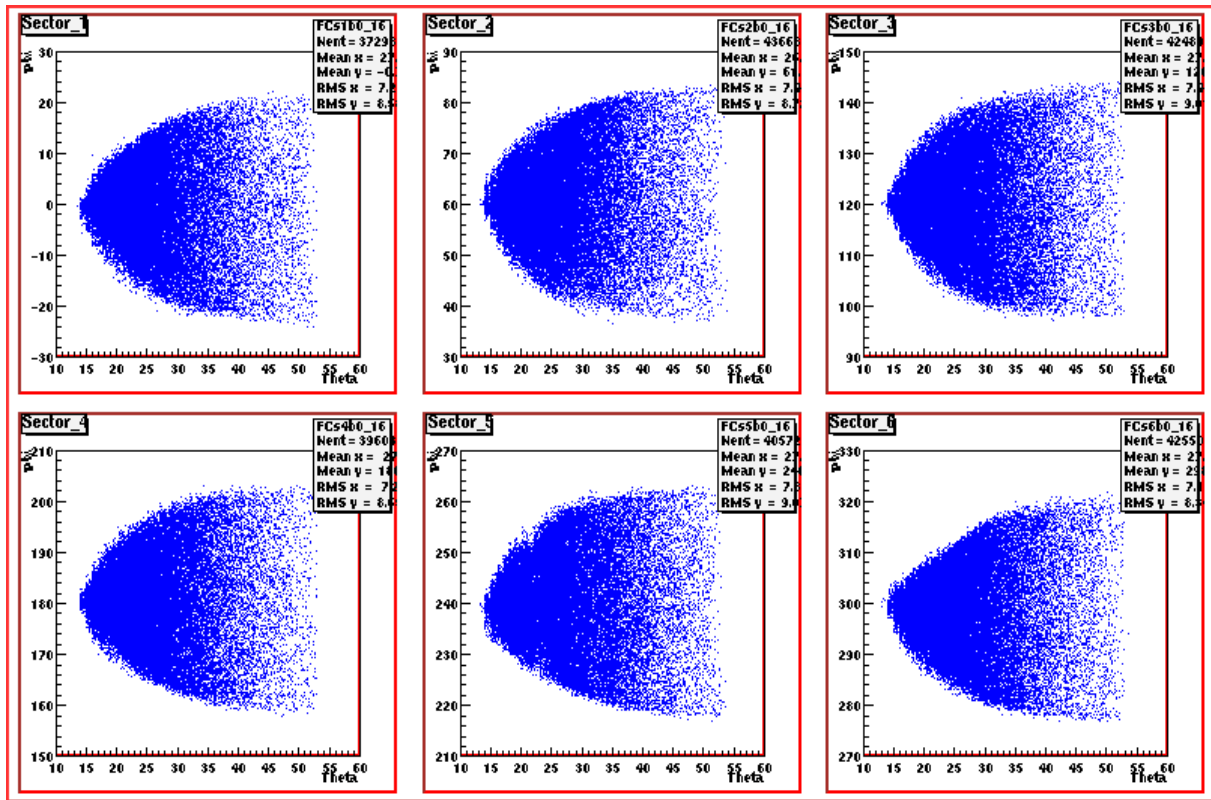


Figure 11: Overall result of the cut. One can see that an asymmetrical shape resulted in some sectors. The fuzzy edges are due to bin overlap.

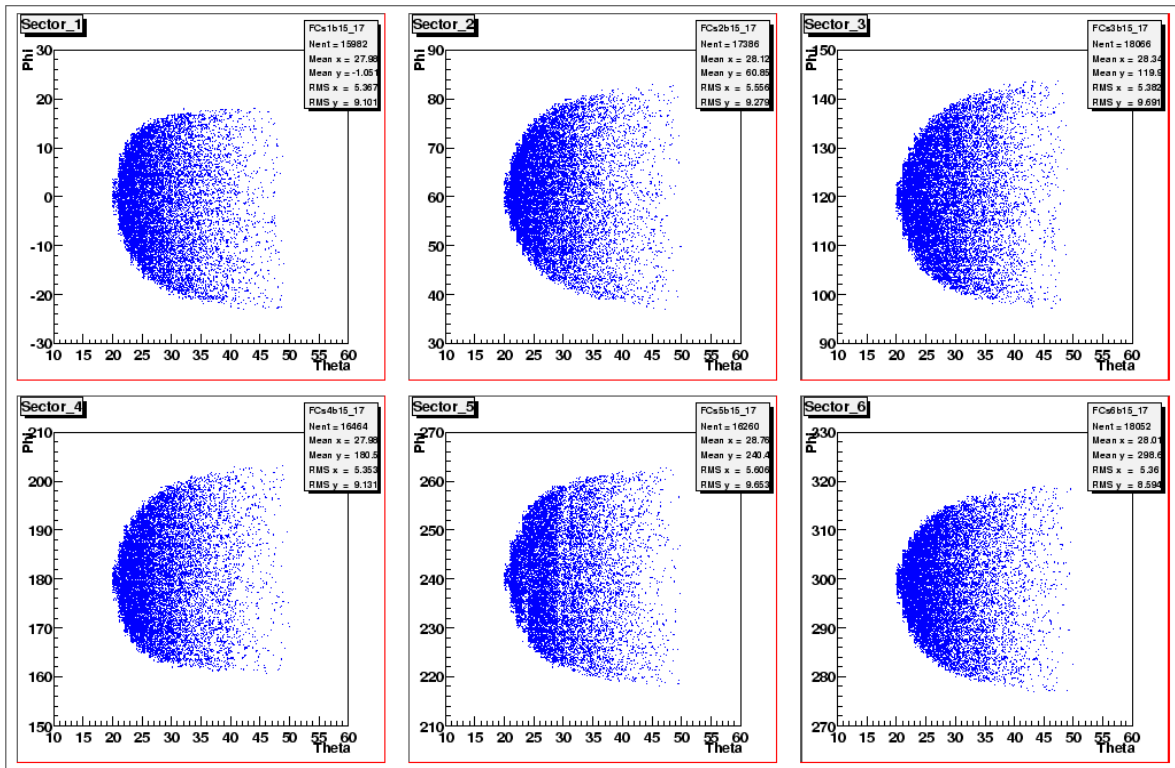


Figure 12: Typical plots illustrating the result of the cut. Please notice that some are asymmetrical. For more, please consult [7]

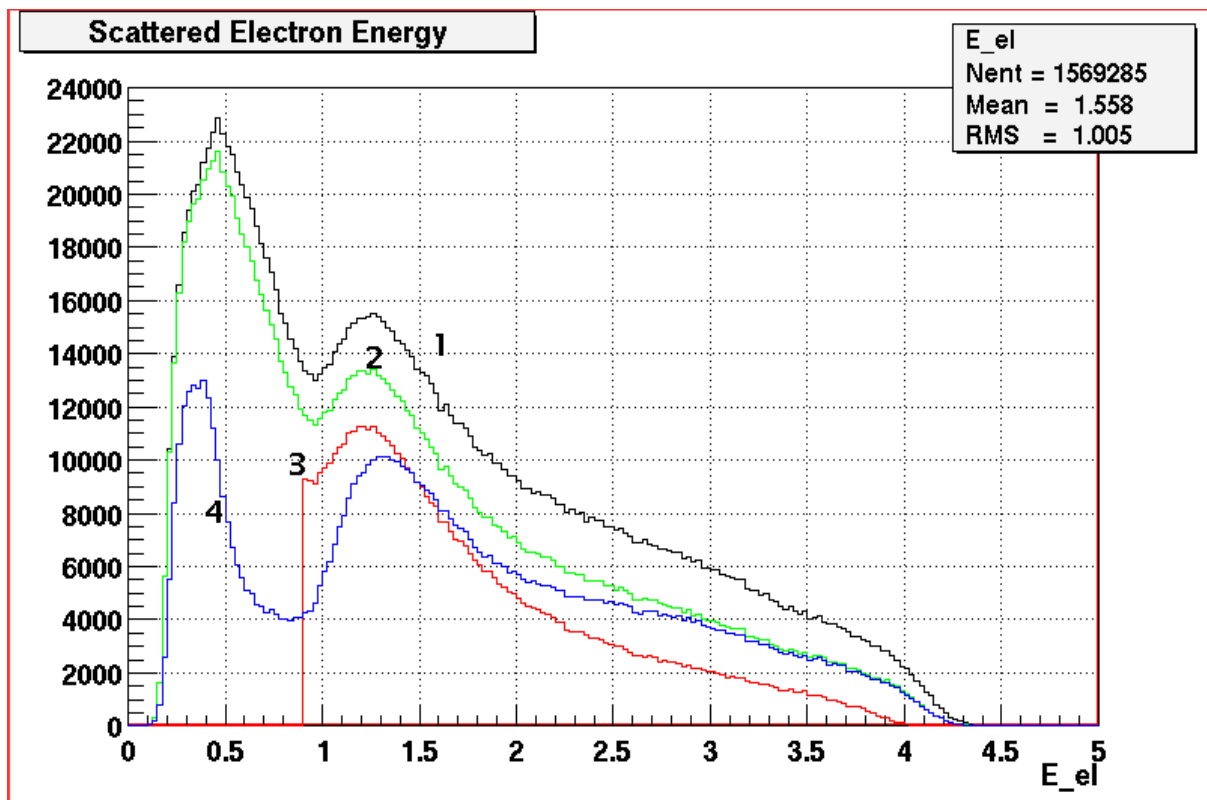


Figure 13: Electron energy spectra at various stages of the procedure: before applying any cut (1), after the  $uvw$  cut (2), after the EC cut on  $uvw$  and  $E/p$  (4), final (3). On the last one, the region  $p < 0.9$  GeV is ignored.  $E_{el}$  is in GeV.